Using Matrix-Assisted Laser Desorption Ionization Mass Spectrometry To Map the Quinol Binding Site of Cytochrome bo_3 from *Escherichia coli*†

Panagiota H. Tsatsos,‡ Kate Reynolds,‡ Elizabeth Furlong Nickels,‡ Da-Yan He,§ Chang-An Yu,§ and Robert B. Gennis*,‡

School of Chemical Sciences, University of Illinois, 600 South Mathews Street, Urbana, Illinois 61801, and Department of Biochemistry and Molecular Biology, Oklahoma State University, Stillwater, Oklahoma 74078

Received April 23, 1998; Revised Manuscript Received June 2, 1998

ABSTRACT: The cytochrome bo_3 ubiquinol oxidase contains at least one and possibly two binding sites for ubiquinol/ubiquinone. Previous studies used the photoreactive affinity label 3-[^{3}H]azido-2-methyl-5-methoxy-6-geranyl-1,4-benzoquinone (azido-Q), a substrate analogue, to demonstrate that subunit II contributes to at least one of the quinol binding sites. In the current work, mass spectroscopy is used to identify a peptide within subunit II that is photolabeled by the azido-Q. Purified cytochrome bo_3 was photolabeled as previously described using azido-Q that was not tritiated (i.e., not radiolabeled). Subunit II was then isolated from an SDS−PAGE gel and proteolyzed in situ with trypsin. The resulting peptides were eluted from the gel and then identified using matrix-assisted laser desorption ionization mass spectrometry. The resulting mass spectrum was compared to that obtained by analysis of subunit II that had not been exposed to the photolabel. Using the amino acid sequence, each peak in the mass spectrum of the unlabeled subunit II could be assigned to an expected trypsin fragment. Two additional peaks were observed in the mass spectrum of the photolabeled subunit with *m*/*z* 1931.9 and 2287.7. Subtraction of the mass of azido-Q from the peak at *m*/*z* 1931.9 results in a mass equivalent to that of a peptide consisting of amino acids 165−178. The assignment of the peak at *m*/*z* 2287.7 cannot be made unequivocally and may correspond either to the covalent attachment of azido-Q to peptide 254−270 or to a peptide resulting from incomplete proteolysis. The labeled peptide, 165−178, is within the water-soluble domain of subunit II, whose X-ray structure is known. This peptide is located near the site where Cu_A is located in the homologous cytochrome *c* oxidases and can be placed near the interface between subunits I and II.

The cytochrome bo_3 ubiquinol oxidase is a member of the heme−copper oxidase superfamily (*6*). It is present when the cells are grown at high oxygen tension and catalyzes the two-electron oxidation of ubiquinol-8 and the four-electron reduction of dioxygen to water (*11*, *14*). Cytochrome bo_3 is an integral membrane protein consisting of one copy each of four subunits, I (74.4 kDa), II (34.9 kDa), III (22.6 kDa), and IV (12.0 kDa), encoded by the *cyo*ABCDE operon (*2*). The genes encode subunits II (*cyo*A), I (*cyo*B), III (*cyo*C), and IV (*cyo*D). *Cyo*E encodes a farnesyltransferase required for the biosynthesis of heme O (*18*−*20*).

A photoreactive radiolabeled ubiquinol analogue, 3-[^{3}H]-azido-2-methyl-5-methoxy-6-geranyl-1,4-benzoquinone (azido-Q), was used recently to show that subunit II was involved in the binding of ubiquinol (*28*). Azido-Q, when reduced by dithiothreitol, functions as a substrate, suggesting that it interacts at a legitimate ubiquinol binding site. Upon photolysis, a nitrene form of the label is produced which covalently inserts into the protein. SDS−PAGE analysis showed that subunit II was the primary target of the label. In the current work, this study is extended by using matrix-assisted laser desorption ionization (MALDI) mass spectrometry to identify a peptide within subunit II that is labeled by the azido-Q photolabel. The data suggest that a ubiquinol binding site of cytochrome bo_3 is located at the interface between subunits I and II.

MATERIALS AND METHODS

Purification of Cytochrome bo_3. Histidine-tagged cytochrome bo_3 oxidase was purified on a Qiagen Ni^{2+}−NTA resin low-pressure affinity column as described by Rumbley et al. (*17*).

Enzyme Activity Assay. The enzymatic activity of the cytochrome bo_3 enzyme was determined by following the O_2 uptake using ubiquinol-1 as substrate at 37 °C using a YSI Model 53 oxygen electrode. The assay mixture contained 50 mM HEPES buffer, pH 7.5, 0.01% dodecyl maltoside, and 2 mM dithiothreitol. The concentration of ubiquinol-1 used was 245 μM.

Ubiquinol Content of Cytochrome bo_3. The quinol content of the enzyme was determined as described previously, using an organic extraction followed by separation by HPLC (*17*).

Photolabeling of Cytochrome bo_3. The photoreactive azidoubiquinone derivative 3-azido-2-methyl-5-methoxy-6-

† Supported by grants from the U.S. Department of Energy, DEFG-02-87ER13716 (R.B.G.), and the NIH, GM30721(C.-A.Y.).

* Corresponding author: tel, 217-333-9075; fax, 217-244-3186; e-mail, R-Gennis@UIUC.edu.

‡ University of Illinois.

§ Oklahoma State University.

S0006-2960(98)00927-1 CCC: $15.00
Published on Web 06/23/1998

geranyl-1,4-benzoquinone (azido-Q) was synthesized as previously described (*28*). For this study, the azido-Q was not radiochemically labeled. Cytochrome bo_3 (25 μM in 50 mM phosphate buffer, pH 7.8, with 0.05% sodium cholate) was placed in a quartz cuvette which was incubated at 4 °C in a cold box. An 8-fold molar excess of azido-Q was added to the protein solution and subjected to UV illumination for 20 min with a UVP Inc. Model UVL-56 long-wave UV lamp as in the previous study (*28*).

SDS−PAGE. Samples containing 40 μg of protein were incubated in SDS−PAGE sample buffer (five times) for 30 min at room temperature. SDS−PAGE analysis was performed as described by Laemmli (*12*) using a 10% Tris−glycine precast Ready Gel from Bio-Rad with a 4% stacking gel. The gel was run for 45 min at 175 mA in the Bio-Rad mini-PROTEAN II electrophoresis system. The gel was stained for 30 min in Coomassie Blue-R250 stain containing 10% acetic acid, 40% methanol, and 0.1% Coomassie R-250 and then destained three times for 30 min each with a solution containing 10% acetic acid and 40% methanol.

In Situ Proteolysis. Subunit II of cytochrome bo_3, which was previously shown to bind to azido-Q, was cut from the gel and subjected to trypsin digestion in situ (*13*). Trypsin was added in a 1:25 weight-to-weight ratio of protease to protein and incubated at 37 °C for 24 h. The peptides were then isolated as described (*13*) and analyzed by mass spectrometry.

Matrix-Assisted Laser Desorption Ionization. Molecular mass determination was done using the matrix-assisted laser desorption ionization (MALDI) technique with a laser desorption VG time-of-flight spectrometer. The matrix used was α-cyano-4-hydroxycinnamic acid which was purchased from Sigma. One to five picomoles of protein embedded in the matrix was placed on the target and dried. Once a spectrum was obtained, assignment of peaks was accomplished by using BioLynx Peptide Analysis software from Micromass Inc.

Molecular Modeling. A full atomic structure was generated using the program MODELLER (*21*). The protein sequences of subunits I, II, and III of cytochrome bo_3 were aligned to the known structures from bovine heart mitochondria (*25*, *26*) and *Paracoccus denitrificans* (*10*) using GCG (*8*). Regions of cytochrome bo_3 with low homology to the cyctochrome *c* oxidases, i.e., helices 0, XIII, and XIV in subunit I, were truncated. The prosthetic groups were manually aligned since reference parameters were unavailable. The coordinates for ubiquinone were taken from the structure of the photosynthetic reaction center [PDB code 1PRC (*1*)]. The ubiquinone was then manually docked using the program VMD (*9*) in the region of the peptide which was indicated by mass spectrometry as being at the azido-Q binding site.

RESULTS

Photolabeling of cytochrome bo_3 with azido-Q resulted in 30% inhibition of the ubiquinol-1 oxidase activity, similar to that which was observed previously with the radiochemically labeled azido-Q. Since the label was shown previously to be covalently attached to subunit II, this subunit was resolved from the other polypeptides by SDS−PAGE (*28*).

In situ digestion of subunit II of both photolabeled enzyme and the control (not photolabeled) with trypsin produced a number of completely digested in addition to partially digested peptides which were analyzed by using MALDI. Figure 1 shows the mass spectra of samples derived from identically treated gel slices that contained no protein (not shown), subunit II which was not photolabeled (trace B), and subunit II which was photolabeled (trace A). The mass spectrum of the sample containing no protein was subtracted from each of the mass spectra shown in Figure 1. Peaks in these spectra were assigned using BioLynx Peptide Analysis software (Table 1). Not all peptides were detected due to the limitation of MALDI to detect a mass close to the molecular weight of the organic matrix used. In the mass spectrum of the photolabeled protein there are two peaks, at *m*/*z* 1930.9 and at *m*/*z* 2287.7, that are not present in the spectrum of the subunit that was not photolabeled. These two peaks were observed consistently in independently photolabeled preparations of the enzyme. It is assumed that one or both of these new peaks could be the result of a change in mass due to the covalent attachment of azido-Q to a specific peptide. There is no peptide that corresponds to a *m*/*z* of 1930.9 (Table 1), and this peak is interpreted as due to azido-Q (expected mass 329.4) covalently attached to peptide 165−178 (expected mass 1597.7). The assignment of peak *m*/*z* 2287.7 is less clear. This peak could result from a partially digested peptide consisting of amino acids 220−240. Alternatively, the *m*/*z* 2287.7 peak might be due to azido-Q covalently attached to a peptide consisting of amino acid residues 254−270. It is not possible distinguish between these two possibilities. Note that the mass of each of the four expected fragments that constitute peptide 220−240 is too small to detect using MALDI. The peak corresponding to *m*/*z* 2175.5 is assigned to the multiply charged ion of trypsin used to digest the sample.

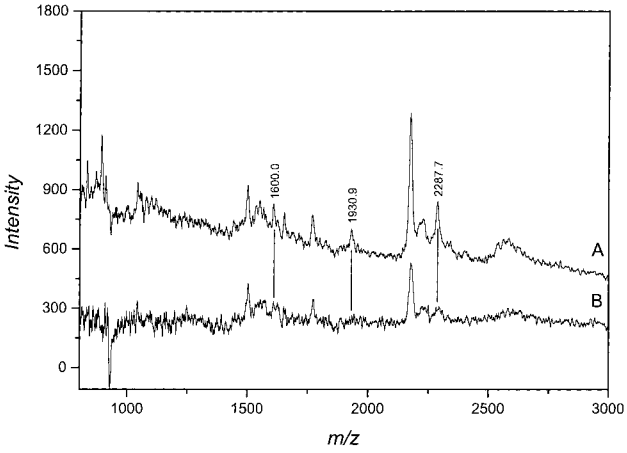

FIGURE 1: MALDI mass spectra of a trypsin digest of subunit II of cytochrome bo_3. trace A shows the results with a sample isolated from an enzyme preparation that had been photolabeled, and trace B shows the corresponding spectrum from enzyme that had not been photolabeled with azido-Q. A control spectrum, treated identically but containing no protein, was subtracted from each of the spectra displayed. The two peaks that are unique to the photolabeled samples are shown at *m*/*z* 1930.9 and 2287.7. The peak at *m*/*z* 1600.0 is assigned to the peptide corresponding to residues 165−178 in the absence of the label. See text for details and Table 1 for a list of assignments.

The X-ray structure of the water-soluble domain of subunit II of cytochrome bo_3 is known (*29*), and peptides 165−178 and 254−270 are both within this domain (Figure 2). These two peptides are sufficiently close to each other at some

Table 1: Assignment of Peptides Observed by MALDI-TOF of Trypsin Digestion of Subunit II of Cytochrome bo_3 Oxidase

residues	average mass, Da		
	measured	calculated	difference
25[a]−33			
34−41	903.6	899.0	4.6
42−68	2890.0	2887.7	2.3
69−70	ND[b]	336.4	
71−74	ND	417.4	
75−77	ND	331.4	
78−87	1222.3	1218.3	4.0
88−109	2534.5	2530.1	4.4
110−118	983.1	982.1	1.0
119−125	ND	807.9	
126−137	1415.9	1416.7	−0.8
138−164	3160.5	3162.6	−2.2
165−178	1600.0	1597.7	2.3
179−192	1528.4	1525.8	2.6
193−219	2774.7	2770.0	4.7
220−221	ND	292.4	
222−228	ND	741.8	
229−237	1037.6	1034.5	3.1
238−239	ND	216.3	
240−253	1556.2	1555.7	0.5
254−270	1961.6	1958.1	3.5
271−280	1131.0	1131.3	−0.3
281−286	ND	688.8	
287−321	4150.1	4154.5	−4.4

[a] Residue is postranslationally modified. ND denotes peptides that were not detected.

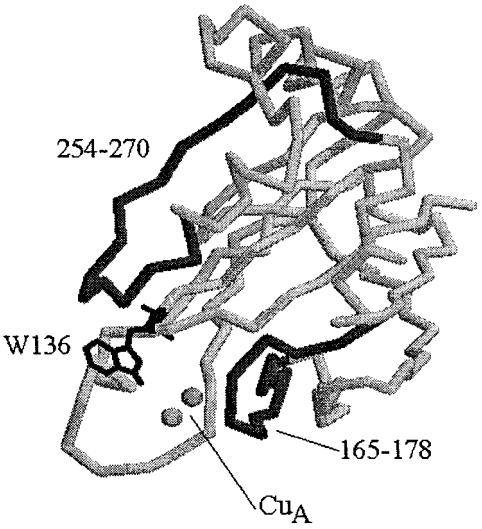

FIGURE 2: Crystal structure of the soluble domain from subunit II of cytochrome bo_3 with an engineered Cu_A site (*29*). The labeled peptides corresponding to residues 165−178 and 254−270 and W136 are highlighted in black.

points (Figure 2), so it is possible that both peptides could be labeled by azido-Q bound to a single binding site. A second possibility is that the two peptides are labeled by azido-Q binding at two different sites, which have been deduced to exist in the enzyme (*23*). Finally, the identification of peptide 254−270 may be an artifact due to incomplete proteolysis, possibly the result of changes induced by the binding of azido-Q to the first site (peptide 165−178).

It is noted that there is substantial evidence supporting the presence of two sites for ubiquinol binding in cytochrome bo_3 (*15*, *22*, *23*). However, the preparation used for this study, as well as the previous labeling with azido-Q (*28*), used enzyme that is associated with about 1 equiv of

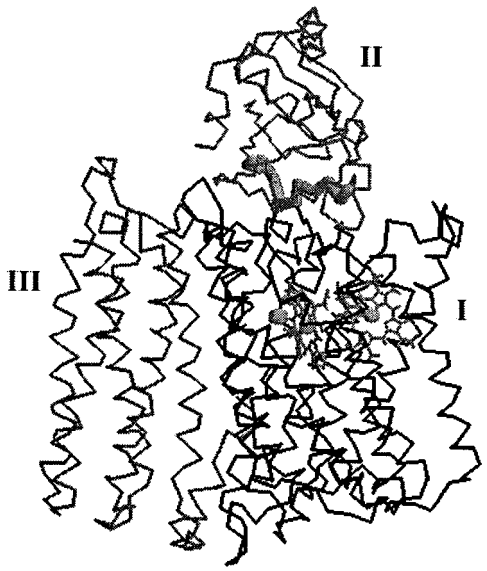

FIGURE 3: Model of subunits I, II, and III of cytochrome bo_3. Subunits I and III were constructed on the basis of the crystal structures of the corresponding subunits from the oxidase from *P. denitrificans* (*10*) and from bovine cytochrome *c* oxidase (*25*, *26*). Subunit II includes the crystal structure of the soluble domain of cytochrome bo_3 as determined by Wilmanns et al. (*29*). The peptide corresponding to residues 165−178 in subunit II is highlighted and shown to be near the interface of subunits I and II. The metal centers in subunit I are shown.

ubiquinone-8. The preparation of the enzyme used in the current work contained about 1.5 equiv of ubiquinol per enzyme molecule. It is expected that one of the quinol binding sites (low-affinity site) would readily exchange with the unbound quinol, whereas the ability of the azido-Q to exchange into the high-affinity site under the experimental conditions utilized is not known.

In cytochrome bo_3, ubiquinol is oxidized by the metal centers located in subunit I. To judge whether the proposed binding site for quinol is functionally plausible, it is necessary to estimate the location of peptide 165−178 with respect to subunit I. There is no high-resolution structure available for cytochrome bo_3. However, there is a high degree of protein sequence identity between the cytochrome bo_3 quinol oxidase and those of the two cytochrome *c* oxidases whose X-ray structures have been reported (*10*, *16*, *25*, *26*). This makes it possible to model a structure for the quinol oxidase sufficient for the purpose. Although the two structures of the cytochrome oxidases are from evolutionarily distant species, bovine (*25*, *26*) and *P. denitrificans* (*10*, *16*), the RMS deviation is only 1.6 Å for the three subunits forming the catalytic core. The model structure of cytochrome bo_3 (subunits I, II, and III) has an average RMS deviation of 1.9 Å (Figure 3). In the model, the labeled peptide is located near the interface of subunit I. Ubiquinol was placed adjacent to the labeled peptide with the additional criterion that is also near residue W136. Site-directed mutagenesis studies (Ma and Gennis, in preparation) have shown that the W136A mutant has an altered K_m for ubiquinol-1, suggesting proximity to the low-affinity ubiquinol binding site. It is significant, therefore, that W136 is located near the labeled peptide. Furthermore, the equivalent residue (W121) in the cytochrome *c* oxidase from *P. denitrificans* has been shown to be important for electron transfer from cytochrome *c* to

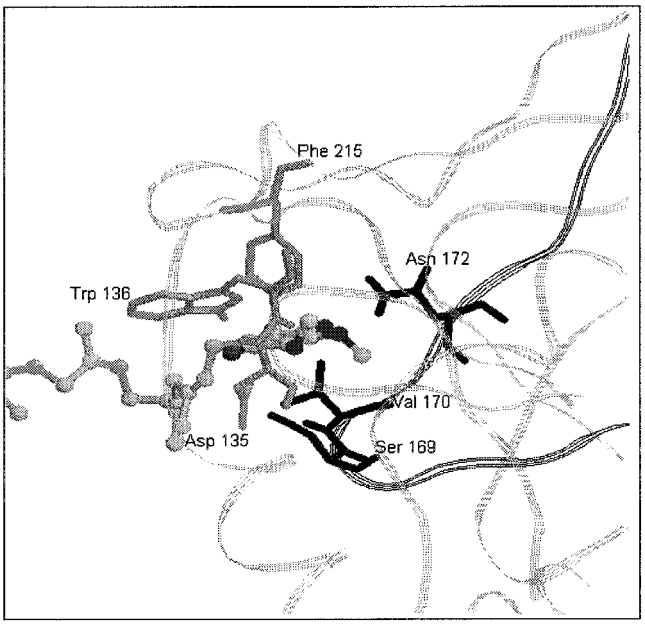

FIGURE 4: Residues within 3.2 Å of the modeled quinol. The ribbon and residues in black correspond to that of labeled peptide 165−178.

Cu_A and is suggested to be the electron entry point into the enzyme (*31*).

The ubiquinol headgroup was manually docked with minimal steric conflicts (see Figure 4). These conflicts were eliminated by minimal movements within the protein or the ubiquinone molecule itself. At this point, the model must be considered an educated guess, providing a basis for the design of future experimentation. With relatively minor adjustments of the model, the bound ubiquinol could be located such that labeling by azido-Q of both peptides 165−178 and 254−270 would be plausible. Residues within 5 Å of the quinol headgroup in subunit II are D135, W136, F215, M218, Y210, N172, V170, M171, S169, and S133. Residues F215, W136, and N172 are within 3 Å in this model, with possible hydrogen bonds to the quinol hydroxyls provided by W136 and N172 (see Figure 4).

DISCUSSION

MALDI mass spectrometry has been used to identify a unique peptide in subunit II of the cytochrome bo_3 ubiquinol oxidase that is covalently labeled with the photoreactive quinol analogue azido-Q. Previous studies using the tritiated photolabel clearly showed that subunit II is the major polypeptide target that became linked to the probe (*28*).

Cytochrome bo_3 is a member of the heme−copper oxidase superfamily and is closely related to the cytochrome *c* oxidases (*6*). In the cytochrome *c* oxidases, subunit II acts as the electron entry point, containing the binding site for the substrate, cytochrome *c*, and also containing the Cu_A redox center, which is the initial electron acceptor from cytochrome *c* (*30*−*32*). Subunit II is anchored to the membrane by two transmembrane helical spans and a large C-terminal hydrophilic domain that essentially sits on top of subunit I and which contains the functionally important residues (*10*, *16*, *25*, *26*). A critical residue modulating the electron transfer from cytochrome *c* to Cu_A is a highly conserved tryptophan in the hydrophilic domain of subunit II (W121 in *P. denitrificans*) (*31*). Reduced Cu_A passes its electron to heme *a* which, in turn, reduces the heme a_3−Cu_B binuclear center, which is the site where dioxygen is reduced to water. Both heme *a* and the heme−copper binuclear center are buried within subunit I of the heme−copper oxidases.

Subunits I, II, and III of the cytochrome bo_3 quinol oxidase are homologous to the equivalent subunits in the cytochrome *c* oxidases, and all the experimental data suggest the same general architecture for these enzymes (*7*). It has long been recognized that subunit II of the quinol oxidases (including cytochrome bo_3) lacks the recognition domain for cytochrome *c* and lacks the Cu_A site as well. The ligands for Cu_A have been restored by site-directed mutagenesis in subunit II of cytochrome bo_3 (*27*), and the structure of the water-soluble domain containing the reconstructed Cu_A has been determined (*29*). The mutant of cytochrome bo_3 containing the reconstituted Cu_A retains quinol oxidase activity, indicating that the site where Cu_A binds in the cytochrome *c* oxidases does not correspond exactly to a quinol binding site in the quinol oxidase (*27*). However, it remains an attractive notion that the general role of subunit II in the quinol oxidases is to provide an electron entry point for the enzyme and a site for quinol oxidation analogous to the cytochrome *c*/Cu_A sites in the cytochrome *c* oxidases. This idea is supported by the photolabeling of subunit II by azido-Q (*28*).

The current work locates a quinol binding site near peptide 165−178. The parallel program of site-directed mutagenesis of conserved residues in subunit II revealed W136 as possibly being near the exchangeable quinol binding site. Interestingly, W136 is the equivalent to W121, the "electron entry point" in the cytochrome *c* oxidase from *P. denitrificans* (*31*). W136 and peptide 165−178 are near each other in subunit II of cytochrome bo_3 (Figure 2) and provide a rational basis for building a model to approximate the quinol binding site. This site is located quite close to the "Cu_A site" ($\simeq$3 Å), though not overlapping, and is also near the interface of subunits I and II and, thus, can conceivably be accessed by the membrane-bound ubiquinol-8 substrate. The ubiquinol binding site is also close to the second peptide identified in this work, peptide 254−270, though it is not certain that this peptide is labeled by azido-Q at the same binding site.

The best defined structures of protein-bound ubiquinone are those of the bacterial photosynthetic reaction centers (*3*−*5*, *24*). The polyisoprene chains in the quinones bound to different sites in the photosynthetic reactions centers are observed in distinct configurations, and the headgroups are completely buried within the protein. Interestingly, there is no clear pathway for the quinone/quinol to enter and exit the exchangeable site in the reaction centers. The substrate must diffuse from the membrane bilayer through the protein to attain its bound configuration. In the case of cytochrome bo_3, the quinol site which is defined by the model (Figure 4) can be accessed from the membrane bilayer by diffusing through a space between transmembrane helices in subunit I, and in the bound configuration with the headgroup within subunit II, the polyisoprene chain would be largely within subunit I. It is reasonable to assume that the site defined by the photoaffinity labeling corresponds to the low-affinity site, which is expected to readily exchange with bulk quinol (*15*, *22*, *23*). The enzyme used in this study has the high-affinity site occupied by ubiquinol-8. However, it cannot be ruled

out that the azido-Q could exchange into the high-affinity site under the experimental conditions used for this work (*15*). Hence, possibly the two peptides identified in this work could represent two different binding sites for ubiquinol. This will be addressed in future studies, which will also be designed to test and refine the model.

ACKNOWLEDGMENT

We express sincere thanks to Jeff Osborne for providing the protein which was used for these experiments and to Dr. Richard Milberg and the University of Illinois at Champaign−Urbana Mass Spectrometry Center.

REFERENCES

1. Abola, E. E., Sussman, J. L., Prilusky, J., and Manning, N. O. (1997) *Methods Enzymol. 277*, 556−571.
2. Chepuri, V., Lemieux, L. J., Au, D. C.-T., and Gennis, R. B. (1990) *J. Biol. Chem. 265*, 11185−11192.
3. Deisenhofer, J., and Michel, H. (1989) *Science 245*, 1463−1473.
4. Ermler, U., Fritzsch, G., Buchanan, S. K., and Michel, H. (1994) *Curr. Biol. 2*, 925−936.
5. Feher, G., Allen, J. P., Okamura, M. Y., and Rees, D. C. (1989) *Nature 339*, 111−116.
6. Garcia-Horsman, J. A., Barquera, B., Rumbley, J., Ma, J., and Gennis, R. B. (1994) *J. Bacteriol. 176*, 5587−5600.
7. Gohlke, U., Warne, A., and Saraste, M. (1997) *EMBO J. 16*, 1181−1188.
8. Genetics Computer Group (1997) *GCG Wisconsin Package*, Version 9.1, Madison, WI.
9. Humphrey, W., Dalke, A., and Sschulten, K. (1996) *J. Mol. Graphics 14*, 33−38.
10. Iwata, S., Ostermeier, C., Ludwig, B., and Michel, H. (1995) *Nature 376*, 660−669.
11. Kita, K., Konishi, K., and Anraku, Y. (1984) *J. Biol. Chem. 259*, 3368−3374.
12. Laemmli, U. K. (1970) *Nature 227*, 680−685.
13. Matsudaira, P. (1993) in *A Practical Guide to Protein and Peptide Purification for Microsequencing* (Matsudaira, P., Ed.) pp 59−61, Academic Press, Inc., San Diego, CA.
14. Minghetti, K. C., and Gennis, R. B. (1988) *Biochem. Biophys. Res. Commun. 155*, 243−248.
15. Musser, S. M., Stowell, M. H. B., Lee, H. K., Rumbley, J. N., and Chan, S. I. (1997) *Biochemistry 36*, 894−902.
16. Ostermeier, C., Harrenga, A., Ermler, U., and Michel, H. (1997) *Proc. Natl. Acad. Sci. U.S.A. 94*, 10547−10553.
17. Rumbley, J. N., Nickels, E. F., and Gennis, R. B. (1997) *Biochim. Biophys. Acta 1340*, 131−142.
18. Saiki, K., Mogi, T., and Anraku, Y. (1992) *Biochem. Biophys. Res. Commun. 189*, 1491−1497.
19. Saiki, K., Mogi, T., Hori, H., Tsubaki, M., and Anraku, Y. (1993) *J. Biol. Chem. 268*, 26927−26934.
20. Saiki, K., Mogi, T., Ogura, K., and Anraku, Y. (1993) *J. Biol. Chem. 268*, 26041−26045.
21. Sali, A. (1995) *Mol. Med. Today 1*, 270−277.
22. Sato-Watanabe, M., Mogi, T., Miyoshi, H., Iwamura, H., Matsushita, K., Adachi, O., and Anraku, Y. (1994) *J. Biol. Chem. 269*, 28899−28907.
23. Sato-Watanabe, M., Mogi, T., Ogura, T., Kitagawa, T., Miyoshi, H., Iwamura, H., and Anraku, Y. (1994) *J. Biol. Chem. 269*, 28908−28912.
24. Stowell, M. H. B., McPhillips, T. M., Rees, D. C., Soltis, S. M., Abresch, E., and Feher, G. (1997) *Science 276*, 812−816.
25. Tsukihara, T., Aoyama, H., Yamashita, E., Takashi, T., Yamaguichi, H., Shinzawa-Itoh, K., Nakashima, R., Yaono, R., and Yoshikawa, S. (1996) *Science 272*, 1136−1144.
26. Tsukihara, T., Aoyama, H., Yamashita, E., Tomizaki, T., Yamaguchi, H., Shinzawa-Itoh, K., Nakashima, T., Yaono, R., and Yoshikawa, S. (1995) *Science 269*, 1069−1074.
27. van der Oost, J., Pappalainen, P., Musacchio, A., Warne, A., Lemieux, L., Rumbley, J., Gennis, R. B., Aasa, R., Pascher, T., Malmström, B. G., and Saraste, M. (1992) *EMBO J. 11*, 3209−3217.
28. Welter, R., Gu, L.-Q., Yu, L., Yu, C.-A., Rumbley, J., and Gennis, R. B. (1994) *J. Biol. Chem. 269*, 28834−28838.
29. Wilmanns, M., Lappalainen, P., Kelly, M., Sauer-Eriksson, E., and Saraste, M. (1995) *Biochemistry 34*, 11955−11959.
30. Witt, H., Malatesta, F., Nicoletti, F., Brunori, M., and Ludwig, B. (1998) *FEBS Lett. 251*, 367−373.
31. Witt, H., Malatesta, P., Nicoletti, F., Brunori, M., and Ludwig, B. (1998) *J. Biol. Chem. 273*, 5132−5136.
32. Witt, H., Wittershagen, A., Bill, E., Kolbesen, B. O., and Ludwig, B. (1997) *FEBS Lett. 409*, 128−130.

BI9809270